Quaternion Screened Poisson Equation for Low-Light Image Enhancement

Chaoyan Huang ⓘ, Yingying Fang ⓘ, Tingting Wu ⓘ, Tieyong Zeng ⓘ, and Yonghua Zeng

Abstract—Image enhancement is a technique to enhance the illumination of dark images while keeping the reality and the naturalness of the enhanced images at the same time. For color images, most methods tackle different color channels in a separate way, which overlooks the connection between the color channels. Therefore, in this letter, we consider a quaternion-based model to reserve the color connectivity, which integrates the color information of a pixel by a quaternion number. Moreover, we propose a regularizer based on the gamma-correction function and incorporate it into a screened Poisson equation for the image enhancement task. The uniqueness and existence of the solution of the proposed model are analyzed. The numerical results also prove the superiority of our scheme for color image enhancement.

Index Terms—Image enhancement, quaternion analysis, gamma-correction, screened Poisson equation.

I. INTRODUCTION

IMAGES are one of the most important carriers for people to acquire information. However, due to the limitation of the imaging devices, it is easy to get underexposed images in the evenings, cloudy days, or while the fast shutter speed is adopted to avoid the blur [1]–[3]. In these cases, image enhancement is an important post-processing technique to retrieve the contents from the observed dark images, by lifting the contrast and illumination of the observed images [4]–[6].

As a task mainly performed on the color images, we notice that many enhancement methods apply the model of processing grayscale images to color images in a straightforward manner, which could easily lead to the inconsistency between the color channels of the enhanced images. For example, the authors in [7] regarded the color image as a linear combination of three grayscale images and applied the total variation-based model [8] to each image without considering the relationship between the color channels. In [9], Limare *et al.* applied the screened Poisson equation (SPE) to each R, G, B (red, green, blue) channel for the retinex task, and got some color noise in the results. Later, Morel *et al.* [10] utilized the SPE to image enhancement task which handled grayscale images well, however the results also suffered from color distortions since the method was performed on R, G, B channels, independently. These facts showed that it is not enough to treat color images as a simple combination of three gray images, since the restored images will easily have color artifacts or color distortion due to overlooking the color consistency. Additionally, many methods were explored to turn the image from the RGB color space to another space, such as HSV and YCbCr spaces. The authors in [11] proposed a simple but efficient scheme. Instead of treating only the luminance component of color images in YCbCr color space, they also processed chromatic components for preserving the colors. To better save the color information, [12] converted the color image to HSV space. To our understanding, these kinds of methods could therefore handle color images without RGB channels on their own. However, the processing on the transformed channels overlooks the color relations between channels and could bring about the color unreality after enhancement.

Considering the above problems, Pei and Cheng [13] represented the color image by a pure quaternion. A color image u of size $M \times N$ is denoted by a vector $u = [u_r, u_g, u_b]$, where $u_r, u_g, u_b \in \mathbb{R}^{M \times N}$ are the R, G, B channels, respectively. With the quaternion representation, each pixel in u is represented as $\dot{u}_{pq} = u_{pq}^r i + u_{pq}^g j + u_{pq}^b k$, where $p = 1, 2, \ldots, M$ and $q = 1, 2, \ldots, N$ denote the location of the pixel, and i, j, k are three imaginary units. The details are introduced in Section II-A. Representing a color image as vector, the image is divided into three gray images. While using a quaternion to represent each color pixel, the color information and cross-channel information are all reserved as an inseparable quaternion number. Considering the properties of the quaternion, several works have emerged to extend traditional restoration models into the quaternion domain [14]–[19]. Their works showed that models based on the quaternion are more effective in preserving color structures, which means it is promising to apply the quaternion to enhance the color images.

In this letter, we introduce a quaternion-based image enhancement model established from the SPE. As the regularizer is a potent tool to handle the ill-posed tasks, we also extend the gamma correction into the quaternion domain as a regularizer. The *contributions* of this letter can be summarized as follows:

- An image enhancement model based on the quaternion is proposed. To the best of our knowledge, it is the first enhancement model using the pure quaternion representation. Experimental results prove its superiority in enhancing the

Chaoyan Huang, Yingying Fang, and Tieyong Zeng are with the Department of Mathematics, The Chinese University of Hong Kong, Hong Kong (e-mail: cyhuang@math.cuhk.edu.hk; 17481201@life.hkbu.edu.hk; zeng@math.cuhk.edu.hk).

Tingting Wu is with the School of Science, Nanjing University of Posts and Telecommunications, Nanjing 210023, China (e-mail: wutt@njupt.edu.cn).

Yonghua Zeng is with the College of Field Engineering, PLA Army Engineering University, Nanjing 210001, China (e-mail: protege_user@126.com).

dark images to ones with more natural brightness than the ones without quaternion.
- We propose an efficient enhancement regularizer with the gamma-correction and apply it with the SPE model. The experiments showcase its validity for image enhancement.
- We derive and give the theoretical analysis to the solution of our model. Experiments on both simulated and real images show that our method has superior performance.

The rest of this letter is organized as follows. In Section II, we review some related works about the quaternion and the SPE. In Section III, the proposed model is given and analyzed. We implement the experiments in Section IV to illustrate the effectiveness of our method. Section V concludes this letter.

II. RELATED WORKS

In this section, we review the quaternion theory and the screened Poisson equation for the image enhancement task to facilitate the understanding of the proposed model.

A. Quaternion Theory

The quaternion was first introduced by Hamilton [20]. Assuming that $\mathbb{H}$ is a quaternion space, a quaternion number $\dot{f} \in \mathbb{H}$ is defined as

$$\dot{f} = f_0 + f_1 i + f_2 j + f_3 k, \tag{1}$$

where $f_0 \in \mathbb{R}$ is the real part, $f_1, f_2, f_3 \in \mathbb{R}$ are the imaginary parts, and i, j, k are imaginary units. When $f_0 = 0$, $\dot{f}$ is called as pure quaternion. Similar to complex numbers, a quaternion imaginary units satisfy $i^2 = j^2 = k^2 = ijk = -1$. However, the imaginary units does not satisfy the commutative law but follows $ij = -ji = k, jk = -kj = i, ki = -ik = j$.

Quaternion was first introduced into color image processing in [13]. They found there are certain relations between color channels. Hence, they treated each pixel of a color image as a whole instead of dividing them into three separate gray images. As imaginary parts of the quaternion have same properties, the color image $u \in \mathbb{R}^{M \times N \times 3}$ with quaternion is given as

$$\dot{u} = \begin{bmatrix} \dot{u}_{11}, \dot{u}_{12}, \dots, \dot{u}_{1N} \\ \dot{u}_{21}, \dot{u}_{22}, \dots, \dot{u}_{2N} \\ \dots \\ \dot{u}_{M1}, \dot{u}_{M2}, \dots, \dot{u}_{MN} \end{bmatrix}, \tag{2}$$

where $\dot{u}_{pq} = u_{pq}^r i + u_{pq}^g j + u_{pq}^b k$, $p = 1, 2, \dots, M$, and $q = 1, 2, \dots, N$, that is, each pixel of the color image is regarded as a pure quaternion number. To further facilitate the calculation, [21] proposed a better way to represent images with quaternion. Similar to the complex space, they assumed that $\mu = \frac{1}{\sqrt{3}}(i + j + k)$ is the unit pure quaternion and any unit quaternion T related to μ has the following expression

$$T = |T| \exp(\mu \theta) = \cos \theta + \mu \sin \theta. \tag{3}$$

With the definition of the conjugation of a quaternion: $\dot{f}^* = f_0 - f_1 i - f_2 j - f_3 k$, we also have

$$\bar{T} = |\bar{T}| \exp(\mu^* \theta) = \cos \theta - \mu \sin \theta. \tag{4}$$

For the pure quaternion pixel $\dot{v} = v_r i + v_g j + v_b k$, we have

$$T\dot{v}\bar{T} = (\cos \theta + \mu \sin \theta)(v_r i + v_g j + v_b k)(\cos \theta - \mu \sin \theta)$$

$$= [\dot{v} \cdot \cos 2\theta] + [2\mu \cdot (\mu \cdot \dot{v}) \cdot \sin^2 \theta] + [(\mu \times \dot{v}) \sin 2\theta]$$

$$:= \dot{v}^{RGB} + \dot{v}^B + \dot{v}^C.$$

Without loss of generality, we set $\theta = \frac{\pi}{4}$. Then a pure quaternion pixel $\dot{v}$ can be expressed as $\dot{v} = \bar{T}(\dot{v}^B + \dot{v}^C)T$. Thus, for the pure quaternion matrix $\dot{u}$, we have

$$\dot{u} = \bar{T}(\dot{u}^B + \dot{u}^C)T. \tag{5}$$

Note that, we will give the proposed model with equation (5).

Following this, [22] gave the derivation rule of the quaternion matrix. Ell *et al.* gave a fast Fourier transform (FFT) based on quaternion [23]. With the continuous improvement of quaternion theory, quaternion-based models have been applied in various image processing tasks [24], [25]. However, most of these works did not give a theoretical analysis to their models or proof of the existence of the solutions.

B. Screened Poisson Equation-Based Image Enhancement

An image contrast enhancement model for the grayscale image was proposed in [9] as follows:

$$\min_u \int_\Omega |\nabla u - \nabla f|^2 dx + \lambda \int_\Omega (u - f_m)^2 dx, \tag{6}$$

where $u, f \in \mathbb{R}^{M,N}$ are the latent image and observed dark image respectively, f_m is the image whose entries equal to the mean value of the image f and λ is a hyperparameter used to trade off these two terms. Ω denotes the image domain and ∇ is the gradient operator. The solution to (6) satisfies the Euler-Lagrange equation as

$$\lambda(u - f_m) - \Delta u + \Delta f = 0, \quad \text{over} \quad \Omega, \tag{7}$$

where Δ is the Laplace operator. Equation (7) can be further converted to the screened Poisson equation (SPE), whose general form is defined as

$$(\Delta - \beta^2)v = -h, \tag{8}$$

where $\beta^2 = \lambda$ and $h = \lambda f_m - \Delta f$. For SPE, β is a constant called "screening," h and v can be real or complex-valued functions. Then, we say that model (6) is based on the SPE and refer (6) as SPE model. For (8), one can obtain the solution efficiently by the FFT. Hence, the solution to (6) is given as $u = \mathcal{F}^{-1}(\frac{-\mathcal{F}(f)}{\mathcal{F}(\nabla) - \beta^2})$, where $\mathcal{F}(\cdot)$ and $\mathcal{F}^{-1}(\cdot)$ are the Fourier transform and its inverse. Their experiments show the efficacy of SPE in image enhancement. Later, [26] modified SPE and achieved better enhancement performance. Albeit these methods perform well on gray images, the results on color images still suffer from color distortion as a result of ignoring the relationship between color channels. To improve the performance of the color image enhancement, in this letter, we represent the color image with a quaternion matrix.

III. THE PROPOSED SCHEME

In order to achieve a better image enhancement effect, we use the quaternion matrix to represent the color image. Specifically, we assign the pure quaternion to represent each color pixel. Assume that $\dot{f}$ is the observed low-light image, then we have $\dot{f} = \bar{T}(\dot{f}^B + \dot{f}^C)T$, where T is the unit quaternion, $\dot{f}^B$ and $\dot{f}^C$ are brightness and chromaticity components of $\dot{f}$ in quaternion

domain. Accordingly, our model $\dot{J}(\dot{u})$ is

$$\min_{\dot{u}} \int_\Omega |\nabla \dot{u} - \nabla \dot{f}|^2 dx + \frac{\lambda}{2} \int_\Omega (\dot{u} - \dot{f}_m)^2 dx + \frac{\eta}{2} \int_\Omega (\dot{u} - \Phi(\dot{f}))^2 dx,$$
(9)

where $\dot{u} = \bar{T}(\dot{u}^B + \dot{u}^C)T$ is the latent image, $\dot{f}_m = \frac{1}{\Omega} \int_\Omega \dot{f} dx$ is the mean of $\dot{f}$, $\Phi(\dot{f}) = f^{2(G*\dot{f})-1}$ is a coarse enhanced image using gamma-correction with G being the Gaussian kernel. We propose to use this prior to regularizing the final enhanced image. Hence, we name the last term as the quaternion-based gamma-correction regularization. With the derivatives of quaternion matrix [22], we can easily solve $\dot{J}(\dot{u})$ as

$$(\lambda + \eta - \Delta)\dot{u} + \Delta\dot{f} - \lambda\dot{f}_m - \eta[\Phi(\dot{f})]^* = 0, \quad (10)$$

where $(\cdot)^*$ denotes the quaternion conjugate. Let $\rho = \lambda + \eta$ and $\dot{g} = -(\Delta\dot{f} - \lambda\dot{f}_m - \eta[\Phi(\dot{f})]^*)$, then (10) can be reformulated as $(\Delta - \rho)\dot{u} = -\dot{g}$, that is the quaternion-based SPE. To give the existence and uniqueness of the solution to (9), we give Definitions III.1, III.2, and III.3 following [27].

Definition III.1: (quaternion function) Given a domain $D \subset \mathbb{R}^4$ and $x = (x_0, x_1, x_2, x_3) \in D$, then we define a quaternion function $\dot{P} : D \to \mathbb{H}$ as $\dot{P}(x) = x_0 + x_1 i + x_2 j + x_3 k$. In fact, the quaternion function can be also viewed as a mapping from the complex domain $G \subset \mathbb{C}^2$ to the quaternion domain $\mathbb{H}$, where $c = (s, t) \in G$, $s = s_0 + s_1 i \in \mathbb{C}$, $t = t_0 + t_1 i \in \mathbb{C}$. The mapping is then given as $\dot{F}(c) = s + tj = (s_0 + s_1 i) + (t_0 + t_1 i)j = s_0 + s_1 i + t_0 j + t_1 k$.

Definition III.2: Define the differential operator of s and t as

$$\frac{\partial}{\partial s} = \frac{1}{2}\left(\frac{\partial}{\partial s_0} - i\frac{\partial}{\partial s_1}\right), \quad \frac{\partial}{\partial t} = \frac{1}{2}\left(\frac{\partial}{\partial t_0} - i\frac{\partial}{\partial t_1}\right) \quad (11)$$

and its conjugate as

$$\frac{\partial}{\partial \bar{s}} = \frac{1}{2}\left(\frac{\partial}{\partial s_0} + i\frac{\partial}{\partial s_1}\right), \quad \frac{\partial}{\partial \bar{t}} = \frac{1}{2}\left(\frac{\partial}{\partial t_0} + i\frac{\partial}{\partial t_1}\right), \quad (12)$$

then we have $\partial_{\dot{F}}$, $\partial_{\bar{F}}$, $\partial_{\dot{F}}\partial_{\bar{F}}$, and $\partial_{\bar{F}}\partial_{\dot{F}}$ as

$$\partial_{\dot{F}} = 2\left(\frac{\partial}{\partial \bar{s}} + j\frac{\partial}{\partial t}\right), \quad \partial_{\bar{F}} = 2\left(\frac{\partial}{\partial s} - j\frac{\partial}{\partial \bar{t}}\right), \quad (13)$$

$$\partial_{\dot{F}}\partial_{\bar{F}} = \partial_{\bar{F}}\partial_{\dot{F}} = 4\left(\frac{\partial^2}{\partial s\partial \bar{s}} + \frac{\partial^2}{\partial t\partial \bar{t}}\right) = \Delta. \quad (14)$$

Definition III.3: (quaternion regular function) If the quaternion function $\dot{F}(x) \in C^1(G)$ satisfies the equation $\partial_x \dot{F} = 0$, then we say $\dot{F}(x)$ is the left regular function in G. The left regular function is referred to as the regular function for short.

Lemma III.1: If $\dot{F}(x)$ is regular in G, then the component functions of $\dot{F}(x)$ are all harmonized within G.

With these definitions and the theory of complex variable functions, the uniqueness theorem of $\dot{J}(\dot{u})$ is as follows.

Proposition III.1: Suppose $\dot{J}(\dot{u})$ is regular in Ω. If $\dot{J}(\dot{u})$ is always equal to zero on the non-empty open set $G_0 \subset \Omega$, then $\dot{J}(\dot{u})$ is always zero in Ω.

Proof: We know that $\dot{J}(\dot{u}) \in C^1(\Omega)$. From (10), we know that $\partial_{\dot{u}}\dot{J}(\dot{u}) = 0$. From Definition III.3, $\dot{J}(\dot{u})$ is a regular function in a non-empty open set G_0. From Lemma III.1 and the infinite degree differentiability of the harmonic function, $\dot{J}(\dot{u}) \in C^\infty(\Omega)$, then $\Delta\dot{J} = \partial_{\dot{u}}\partial_{\dot{u}}\dot{J} = 0$, so $\dot{J}(\dot{u})$ satisfies the Laplace equation in Ω, and each component function of $\dot{J}(\dot{u})$ is

TABLE I
AVERAGE RESULTS WITH PSNR (DB), SSIM, NSS, NIQE, JNBM, BRISQUE, PIQE, CPBD, AND FADE METRIC INDEX[1] ON DATASETS LOL [28] WITH ALL 500 IMAGES AND VV [29] WITH ALL 23 IMAGES. THE BEST RESULT IS HIGHLIGHTED IN BOLD

Dataset	Index	SDCT [11]	SPE [10]	ALGI [12]	LR3M [30]	BIMEF [31]	WithoutQ	Ours
	PSNR ↑	8.85	15.14	15.27	17.28	13.60	17.95	**18.50**
	SSIM ↑	0.3802	0.5923	0.5296	0.3920	0.6474	0.6580	**0.7198**
	NSS ↑	1.3369	1.3630	1.3347	1.3336	1.3256	1.3695	**1.3974**
LOL	NIQE ↓	7.2268	4.5965	7.9213	5.6134	4.7114	4.5383	**3.6553**
	BRISQUE ↓	37.0951	33.6647	32.6157	48.2182	37.3749	29.3699	**28.9097**
	JNBM ↓	6.9428	3.9368	4.9492	5.9268	4.4186	4.3336	**3.6223**
	CPBD ↓	0.8811	0.6730	0.8331	0.7186	0.6898	0.7210	**0.5837**
	FADE ↓	0.9282	0.9577	0.9200	1.2147	1.2239	1.1196	**0.8632**
	NSS ↑	1.3331	1.3683	1.3638	1.3528	1.3490	1.3837	**1.3866**
	NIQE ↓	2.4530	2.5874	2.4688	3.6595	3.5248	2.3858	**2.3291**
VV	BRISQUE ↓	30.2320	32.0553	28.5775	34.4213	29.3632	27.5903	**27.5038**
	PIQE ↓	39.4223	33.7005	34.5491	65.2651	37.6559	34.7643	**33.6067**
	CPBD ↓	0.6976	0.7386	0.6951	0.7109	0.7224	0.6977	**0.6822**
	FADE ↓	0.8503	1.3757	0.7902	0.7640	0.8102	0.8989	**0.7570**

[1]The codes of the index are downloaded from https://github.com/xialeiliu/RankIQA and https://github.com/steffensbola/blind_iqa_contrast.

TABLE II
AVERAGE RESULTS WITH PSNR (DB) AND NIQE INDEX ON THE TESTSET OF LOL AND VV. THE BEST RESULT IS HIGHLIGHTED IN BOLD

Dataset	Index	RetinexNet [28]	Ours
LOL	PSNR ↑	16.77	**18.50**
	NIQE ↓	8.8785	**3.6553**
VV	NIQE ↓	2.7012	**2.3291**

a harmonic function in G. Hence, if the harmonic function $\dot{J}(\dot{u})$ is zero on G_0, it must always be zero on Ω. ∎

According to Proposition III.1 and $\partial_{\dot{u}}\dot{J}(\dot{u})$ (10), we have the unique solution to model (9) as

$$\dot{u} = \frac{\Delta\dot{f} + \lambda\dot{f}_m + \eta[\Phi(\dot{f})]^*}{\Delta + \lambda + \eta}. \quad (15)$$

IV. EXPERIMENT

To demonstrate the effectiveness of the proposed method, we compare our approach to other enhancement methods including SDCT [11], SPE [10], ALGI [12], LR3M [30], BIMEF [31] on the synthetic low-light images from the paired LOL dataset [28] and the real-world low-light images from the unpaired VV dataset [29]. To validate the efficiency of our quaternion representation and gamma-correction regularizer, we also compare it with the model removing the quaternion representation (WithoutQ) and the quaternion-based gamma-correction regularization (WithoutG), respectively. The enhanced results are measured by both objective numerical metrics and the subjective perceptual quality metric.

A. Experimental Results

Examples of the enhanced images are given in Figs. 1 and 2. Moreover, the numerical results are listed in Table I, which are the average results of 500 paired images in LOL dataset and 23 unpaired images in VV dataset. We choose default parameters given in their codes for compared methods. For the pre-trained network [28], which is trained on the LOL dataset. We list the results in Table II. For our models, the hyper-parameters are chosen by trial and error to produce the best possible results. Specifically, the visual quality and NIQE results of different parameters are present in Fig. 3. More specifically, the parameters are fixed as $\lambda = 10$ and $\eta = 10$ for the LOL dataset and $\lambda = 1$ and $\eta = 10$ for the VV dataset.

(a) Input   (b) SPE 15.32/3.7504   (c) ALGI 14.09/8.1431   (d) RetinexNet 17.55/3.0447   (e) LR3M 13.65/4.3060

(f) BIMEF 15.41/4.1827   (g) WithoutG 19.89/3.8669 (h) WithoutQ 20.40/4.0164   (i) Ours 23.62/2.9551   (j) Ground truth
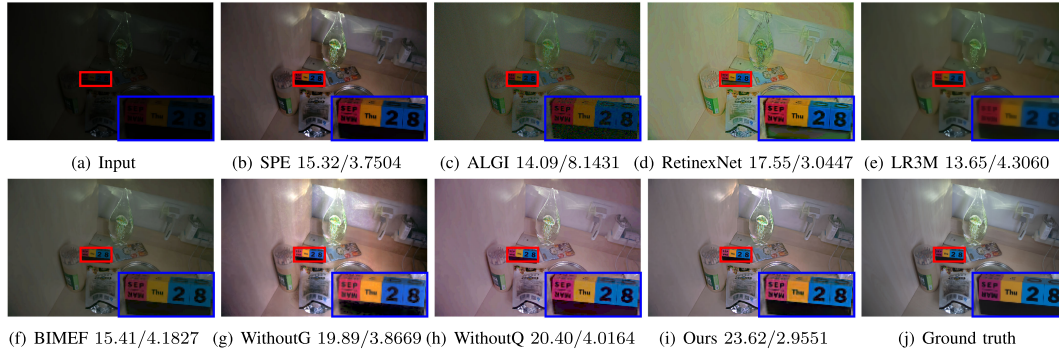
Fig. 1. Comparisons (PSNR↑/NIQE↓) of the proposed model, the proposed model removing quaternion-based gamma-correction (WithoutG), and the proposed model removing quaternion representation (WithoutQ) with SPE [10], ALGI [12], RetinexNet [28], LR3M [30], and BIMEF [31] on the LOL [28] dataset.

(a) Input   (b) SDCT 2.4114   (c) SPE 2.3356   (d) ALGI 2.3218

(e) RetinexNet 2.5887(f) BIMEF 2.3485 (g) WithoutQ 2.3215 (h) Ours 2.2447
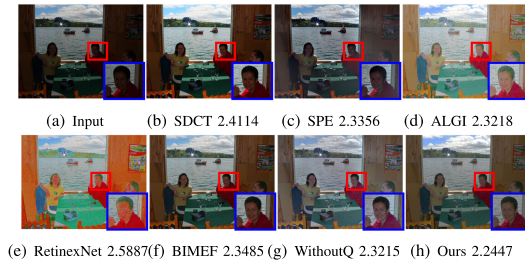
Fig. 2. Comparison (NIQE↓) of the proposed scheme and our method without quaternion (WithoutQ) with SDCT [11], SPE [10], ALGI [12], RetinexNet [28], and BIMEF [31] on the real-world image.

(a) $\beta = 10, \lambda = 0.1$ (b) $\beta = 10, \lambda = 1$ (c) $\beta = 10, \lambda = 20$ (d) $\beta = 10, \lambda = 100$ (e) Input

(f) $\beta = 0.1, \lambda = 10$ (g) $\beta = 1, \lambda = 10$ (h) $\beta = 20, \lambda = 10$ (i) $\beta = 100, \lambda = 10$ (j) Curves
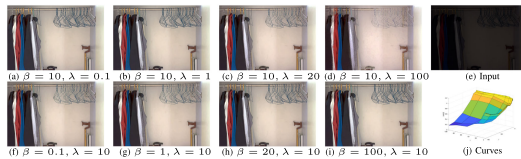
Fig. 3. Analysis of parameters λ and β. (a)–(d) are results with β fixed as 10; (f)–(i) are results with λ fixed as 10; The last column: (e) is the observed low-light image, (j) are the NIQE results with λ and β in $[0.1, 0.2, 0.5, 1, 5, 10, 20, 50, 80, 100]$, respectively.

As one can see, the results of the proposed method have the best visual quality as well as the best numerical metrics. For the results of SPE in Fig. 1, the bright spots in the dark images become outliers while other areas still stay relatively dark. The results of ALGI average the bright spots with the darkness. Adversely, the learning-based method [28] has global overexposed effects with color distortion. On the contrary, the non-local method [30] and variational model [31], both show the limited enhancement performance. Compared to these methods, the proposed model without quaternion (WithoutQ) or the quaternion-based gamma-correction regularizer (WithoutG) reaches a significant improvement in the enhancement performance. However, they are both inferior to the one of the proposed models in Fig. 1(i) adopting both quaternion representation and quaternion-based gamma-correction regularizer, which reaches the most realistic color. For the real-world images, our method in Fig. 2(h) also has the best result. The results of SDCT and SPE show light enhancement effects. On the contrary, the results of ALGI and RetinexNet seem to be over enhanced. For our WithoutQ, one can see that the image is distorted. The numerical results in Tables I and II also prove that the proposed method achieves the best performance in the enhancement tasks.

Besides, the running time of our model varies with image size. It takes an average of 1.52 seconds to enhance an image of size $400 \times 600 \times 3$ in the LOL dataset and 54.65 seconds for an image of size $2304 \times 1728 \times 3$ in the VV dataset.

B. Discussion

Recently, the deep learning-based image enhancement methods almost deserve everyone's attention. Most of them achieve state-of-the-art results at the time. Among them, MIRNet [32] proposes parallel multi-scale convolution streams to extract multi-resolution features. KinD [33] is a classical decomposing network, which introduces degradation removal in the reflectance to improve the quality. DRBN [34] restores the signal based on the fidelity with the supervised dataset and then enhances the results with unsupervised images. SICE [35] learns a contrast enhancer from multi-exposure images. GLAD [36] is able to calculate global illumination and has global illumination-aware, which better handles a wide range of light levels.

Obviously, all the image enhancement networks achieve a significant visual quality improvement for low-light images. However, they rely heavily on large training datasets. Moreover, as these methods are black-boxes, their results lack interpretability [37]. On the contrary, the model-based methods like the proposed one, do not utilize a large number of images for training and work fairly for any given image. The results can be tuned for any given data with its characteristics with good interpretability. In the future work, we will apply the proposed idea to the learning-based model and improve the model interpretability for color image enhancement task.

V. CONCLUSION

In this letter, we proposed a quaternion-based model for low-light image enhancement with the consideration of the inner relationships between color channels. To improve the effectiveness of the enhancement task, we introduced a quaternion-based gamma-corrected regularizer to the screened Poisson equation. Based on the quaternion analysis and the complex variable function theory, we further analyzed the existence and uniqueness of the solution to the proposed model. Experiments proved our scheme reaches the best enhancement performance with the most realistic colors. However, since our method is designed to preserve the color information, it exhibits superior performance on color images but sub-optimal performance on images containing less color information. In the future, we will extend it with data-driven methods.

REFERENCES

[1] J. Tang, E. Peli, and S. Acton, "Image enhancement using a contrast measure in the compressed domain," *IEEE Signal Process. Lett.*, vol. 10, no. 10, pp. 289–292, Oct. 2003.

[2] H. Lee, K. Sohn, and D. Min, "Unsupervised low-light image enhancement using bright channel prior," *IEEE Signal Process. Lett.*, vol. 27, pp. 251–255, 2020.

[3] K. Mei, J. Li, J. Zhang, H. Wu, J. Li, and R. Huang, "Higher-resolution network for image demosaicing and enhancing," in *Proc. IEEE/CVF Int. Conf. Comput. Vis. Workshop*, 2019, pp. 3441–3448.

[4] J. Yao *et al.*, "Deepprognosis: Preoperative prediction of pancreatic cancer survival and surgical margin via comprehensive understanding of dynamic contrast-enhanced CT imaging and tumor-vascular contact parsing," *Med. Image Anal.*, vol. 73, 2021, Art. no. 102150.

[5] J. Li, J. Li, F. Fang, F. Li, and G. Zhang, "Luminance-aware pyramid network for low-light image enhancement," *IEEE Trans. Multimedia*, vol. 23, pp. 3153–3165, 2021.

[6] Q. Yi, J. Li, F. Fang, A. Jiang, and G. Zhang, "Efficient and accurate multi-scale topological network for single image dehazing," *IEEE Trans. Multimedia*, vol. 24, pp. 3114–3128, 2021.

[7] P. Blomgren and T. F. Chan, "Color TV: Total variation methods for restoration of vector-valued images," *IEEE Trans. Image Process.*, vol. 7, no. 3, pp. 304–309, Mar. 1998.

[8] L. I. Rudin, S. Osher, and E. Fatemi, "Nonlinear total variation based noise removal algorithms," *Physica D: Nonlinear Phenomena*, vol. 60, no. 1–4, pp. 259–268, 1992.

[9] N. Limare, A. B. Petro, C. Sbert, and J.-M. Morel, "Retinex poisson equation: A model for color perception," *Image Process. On Line*, vol. 1, pp. 39–50, 2011.

[10] J.-M. Morel, A.-B. Petro, and C. Sbert, "Screened poisson equation for image contrast enhancement," *Image Process. On Line*, vol. 4, pp. 16–29, 2014.

[11] J. Mukherjee and S. K. Mitra, "Enhancement of color images by scaling the DCT coefficients," *IEEE Trans. Image Process.*, vol. 17, no. 10, pp. 1783–1794, Oct. 2008.

[12] H. Chang, M. K. Ng, W. Wang, and T. Zeng, "Retinex image enhancement via a learned dictionary," *Opt. Eng.*, vol. 54, no. 1, 2015, Art. no. 0 13107.

[13] S.-C. Pei and C.-M. Cheng, "A novel block truncation coding of color images using a quaternion-moment-preserving principle," *IEEE Trans. Commun.*, vol. 45, no. 5, pp. 583–595, May 1997.

[14] C. Huang, M. K. Ng, T. Wu, and T. Zeng, "Quaternion-based dictionary learning and saturation-value total variation regularization for color image restoration," *IEEE Trans. Multimedia*, to be published, doi: 10.1109/TMM.2021.3107162.

[15] Y. Yu, Y. Zhang, and S. Yuan, "Quaternion-based weighted nuclear norm minimization for color image denoising," *Neurocomputing*, vol. 332, pp. 283–297, 2019.

[16] Z. Jia, M. K. Ng, and W. Wang, "Color image restoration by saturation-value total variation," *SIAM J. Imag. Sci.*, vol. 12, no. 2, pp. 972–1000, 2019.

[17] C. Huang, Z. Li, Y. Liu, T. Wu, and T. Zeng, "Quaternion-based weighted nuclear norm minimization for color image restoration," *Pattern Recognit.*, vol. 128, 2022, Art. no. 108665.

[18] Z. Jia, Q. Jin, M. K. Ng, and X. Zhao, "Non-local robust quaternion matrix completion for large-scale color images and videos inpainting," *IEEE Trans. Image Process.*, vol. 31, pp. 3868–3883, Jun. 2022.

[19] Z. Jia and M. K. Ng, "Structure preserving quaternion generalized minimal residual method," *SIAM J. Matrix Anal. Appl.*, vol. 42, no. 2, pp. 616–634, 2021.

[20] W. R. Hamilton, "Ii on quaternions; or on a new system of imaginaries in algebra," *London, Edinburgh, Dublin Philos. Mag. J. Sci.*, vol. 25, no. 163, pp. 10–13, 1844.

[21] C. Cai and S. K. Mitra, "A normalized color difference edge detector based on quaternion representation," in *Proc. Int. Conf. Image Process.*, 2000, vol. 2, pp. 816–819.

[22] D. Xu and D. P. Mandic, "The theory of quaternion matrix derivatives," *IEEE Trans. Signal Process.*, vol. 63, no. 6, pp. 1543–1556, Mar. 2015.

[23] T. A. Ell, N. Le Bihan, and S. J. Sangwine, *Quaternion Fourier Transforms for Signal and Image Processing*. Hoboken, NJ, USA: Wiley, 2014.

[24] X. Li, Y. Zhou, and J. Zhang, "Quaternion non-local total variation for color image denoising," in *Proc. IEEE Int. Conf. Syst. Man Cybern.*, 2019, pp. 1602–1607.

[25] Y. Xu, L. Yu, H. Xu, H. Zhang, and T. Nguyen, "Vector sparse representation of color image using quaternion matrix analysis," *IEEE Trans. Image Process.*, vol. 24, no. 4, pp. 1315–1329, Apr. 2015.

[26] P.-W. Hsieh, P.-C. Shao, and S.-Y. Yang, "Adaptive variational model for contrast enhancement of low-light images," *SIAM J. Imag. Sci.*, vol. 13, no. 1, pp. 1–28, 2020.

[27] P. Yang and D. Li, "H_λ-regular vector functions and their boundary value problems," *Boundary Value Problems*, vol. 2012, pp. 1–18, 2012.

[28] C. Wei, W. Wang, W. Yang, and J. Liu, "Deep retinex decomposition for low-light enhancement," in *Proc. Brit. Mach. Vis. Conf.*, 2018, pp. 1–12.

[29] V. Vonikakis, I. Andreadis, and A. Gasteratos, "Fast centre-surround contrast modification," *IET Image Process.*, vol. 2, no. 1, pp. 19–34, 2008.

[30] X. Ren, W. Yang, W.-H. Cheng, and J. Liu, "LR3M: Robust low-light enhancement via low-rank regularized retinex model," *IEEE Trans. Image Process.*, vol. 29, pp. 5862–5876, 2020.

[31] Z. Ying, G. Li, and W. Gao, "A bio-inspired multi-exposure fusion framework for low-light image enhancement," 2017, *arXiv:1711.00591*. [Online]. Available: https://arxiv.org/abs/1711.00591

[32] S. W. Zamir *et al.*, "Learning enriched features for real image restoration and enhancement," in *Proc. Eur. Conf. Comput. Vis.*, 2020, pp. 492–511.

[33] Y. Zhang, J. Zhang, and X. Guo, "Kindling the darkness: A practical low-light image enhancer," in *Proc. 27th ACM Int. Conf. Multimedia*, 2019, pp. 1632–1640.

[34] W. Yang, S. Wang, Y. Fang, Y. Wang, and J. Liu, "From fidelity to perceptual quality: A semi-supervised approach for low-light image enhancement," in *Proc. IEEE/CVF Conf. Comput. Vis. Pattern Recognit.*, 2020, pp. 3063–3072.

[35] J. Cai, S. Gu, and L. Zhang, "Learning a deep single image contrast enhancer from multi-exposure images," *IEEE Trans. Image Process.*, vol. 27, no. 4, pp. 2049–2062, Apr. 2018.

[36] W. Wang, C. Wei, W. Yang, and J. Liu, "Gladnet: Low-light enhancement network with global awareness," in *Proc. 13th IEEE Int. Conf. Autom. Face Gesture Recognit.*, 2018, pp. 751–755.

[37] J. Li, Z. Pei, and T. Zeng, "From beginner to master: A survey for deep learning-based single-image super-resolution," 2021, *arXiv:2109.14335*. [Online]. Available: https://arxiv.org/abs/2109.14335